Observation of a tricyclic[4.1.0.0^{2,4}]heptane during a Michael addition-ring closure reaction and a computational studies on its mechanism of formation

Marco Farren-Dai,[†] John Thompson,[†] Anna Bernardi,[‡] Cinzia Colombo,[†,‡,] Andrew J. Bennet[*,†]*

[†]Department of Chemistry, Simon Fraser University, 8888 University Drive, Burnaby, British Columbia, Canada V5A 1S6; [‡] Università degli Studi di Milano, Dipartimento di Chimica, Via Golgi 19, I-20133 Milano, Italy.

[*]Address correspondence to Andrew J. Bennet, Department of Chemistry, Simon Fraser University, Burnaby, British Columbia, Canada V5A 1S6. Tel: 778-782-8814; Fax: 778-782-3765; E-mail: bennet@sfu.ca

ABSTRACT:

We describe the formation of a bis-cyclopropane product, a tricyclic[4.1.0.0^{2,4}]heptane, that is formed during a Johnson-Corey-Chaykovsky reaction on a cyclopentenone. Two (of four possible) bicyclic products are selectively formed by addition of a COOEt-stabilized sulfur ylide onto the Michael acceptor. The tricyclic product is formed subsequently via a retro Michael elimination of a hindered ether followed by addition of a further cyclopropyl moiety, affecting only one of the two bicyclic products initially formed. The experimental reaction outcome was rationalized using Density Functional Theory (DFT), investigating the different Michael-addition approaches of the sulfur ylide, the transition state (TS) energies for the formation of possible zwitterionic intermediates and subsequent reactions that give rise to cyclopropanation. Selective formation of only two of the four possible products occurs due to the epimerization of unreactive intermediates from the other two pathways, as revealed by energy barriers calculations. The formation of the tricyclic product was rationalized by evaluation of energy barriers for

proton abstraction required to form the intermediate undergoing the second cyclopropanation. The selectivity-guiding factors discussed for single and double cyclopropanation of this functionalized Michael-Acceptor will be useful guidelines for the synthesis of future singly and doubly-cyclopropanated compounds.

INTRODUCTION

Cyclopropanes that contain multiple substituents are important structural motifs present in many agrochemicals, pharmaceuticals and other biologically active compounds.[1-3] Synthesis of such functionalities is challenging due to both the ring strain and the need to control the relative and absolute stereochemistry during synthesis. Among the many synthetic strategies reported, cyclopropanation of electron-rich alkenes is often performed using a transition-metal-catalyzed decomposition of diazoalkanes (diazodecomposition/carbene insertion)[4] or through halomethylmetal (Zn, Sm, Al)-mediated reactions.[5,6] In general, the preparation of cyclopropylcarboxylic acid derivatives involves reacting an alkyl diazoacetate with an alkene using a transition-metal-containing catalyst (i.e., Cu, Co, Ru, Pd, or Rh).[7-9] However, electron-deficient alkenes are normally not reactive under these conditions and for the introduction of functionalized cyclopropyl motifs, a Michael-type addition of a nucleophilic alkylidene reagent is preferable. This reaction, often referred to as a Michael Initiated Ring Closure (MIRC) reaction, involves the conjugate addition of a nucleophile to an electrophilic alkene (conjugated ketones) to produce an enolate intermediate, which undergoes an intramolecular ring closure by displacing the leaving group that is a substituent on the original nucleophile. The usual reagents for this cyclopropane-forming reaction are heteroatom (generally sulfur, phosphorus, arsenic, or tellurium)-containing ylides.[10,11] In particular, the reactivity of sulfur ylides is modulated by electron delocalization from the carbanionic center and by the substituents on the sulfur atom.[12] The reaction of sulfur ylides, initially developed by Johnson,[13] Corey and Chaykovsky,[14,15] has gained increasing attention as such reagents allow ready access to asymmetric cyclopropyl products.[4,11,16-21]

The general mechanism of MIRC reactions involves the stepwise formation of the two C–C bonds (Scheme 1), passing through a zwitterionic intermediate (betaine, **3a** and **3b** in Scheme 1) followed by displacement of the leaving group (SMe_2 in the current study). Depending on the structure of the ylide **1** and the substrate **2**, diastereomeric betaines may result from ylide addition to the substrate. The betaine

intermediate can undergo either direct unimolecular ring closure or bimolecular deprotonation/protonation, resulting in a particular distribution of products (Scheme 1).[22,23]

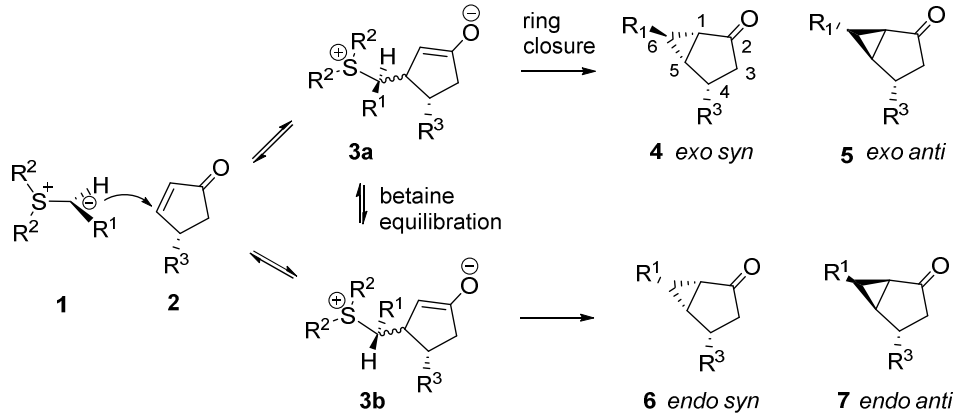

Scheme 1. Cyclopropanation by stepwise Michael addition and ring closure (MIRC) reaction. *Syn*/*anti* refers to relative R_3/cyclopropyl ring configuration. *Endo*/*exo* refers to R_1 configuration, respectively inside or outside the cyclopentyl ring.

Of note, if ketone **2** contains an allylic stereocenter (R_3 in Scheme 1), the facial selectivity of ylide addition yields *anti* or *syn* diastereoisomers in which the cyclopropyl ring and the R_3 substituent are either *trans* or *cis* to each other. The *exo*/*endo* descriptors refer to the configuration of C_6 (R_1) in the diastereomeric product as a result of favored rotation around the C–C bond and/or configurational equilibration of the betaine before the ring closure.[24] The reactivity and the nature of ylides are key factors in determining the reaction path and stereochemical outcome of these cyclopropanation reactions.[4,25] Stabilized sulfur ylides (carbonyl, cyano, sulfonyl and nitro substituted ylides) have been shown to react with the opposite diastereoselectivity to non- or semi-stabilized ylides (alkyl, vinyl or aryl substituted).[26]

In the course of a study to install a cyclopropylcarboxylic acid fused to a functionalized cyclopentenone (Scheme 2)[27] we observed, in addition to the expected bicyclo[3.1.0]hexane derivatives (**10** and **11**, Scheme 2), the formation of a tricyclic product (**12**, Scheme 2). We report a detailed investigation that

demonstrates that conversion to this tricyclic[4.1.0.0^{2,4}]heptyl product requires an excess of sulfur ylide and base. In addition, its formation occurs from one of the two initial bicyclic products. We also report a density functional theory (DFT) reaction coordinate analysis for all possible reaction pathways of this second MIRC reaction. Further, we report an in-depth experimental and theoretical (density functional theory, DFT) study on the formation of this highly functionalized bicyclo[4.1.0.0^{2,4}]heptane.

Scheme 2. Cyclopropanation reaction of enone **8**.

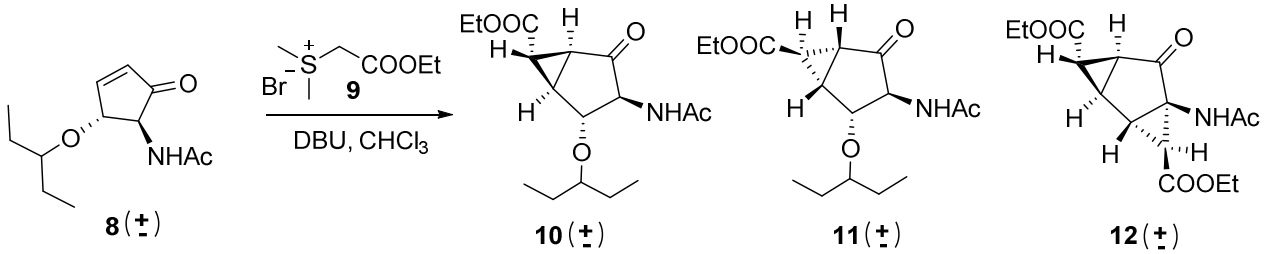

RESULTS AND DISCUSSION

Recently, we reported the application of a Johnson-Corey-Chaykovsky cyclopropanation reaction on a functionalized cyclopentenone **8**, for the preparation of influenza neuraminidase inhibitor candidates.[27] At room temperature in chloroform, an overnight reaction with an enone concentration of 0.08 M and 1.2 equivalent of ethyl (dimethylsulfonium)acetate bromide **9** and DBU (1,8-diazabicyclo[5.4.0]undec-7-ene) gave the two desired bicyclic ketones **10** and **11** (Scheme 2) that were isolated in 30% and 32% yield, respectively. However, analysis of the crude product by ^{1}H-NMR spectroscopy showed no remaining starting material and formation of a third product (see Supporting Information (SI): Figure S1).

We initiated a study to optimize the formation of **10** and **11** by varying the concentrations of the starting materials and the base DBU. Surprisingly, increasing amounts of byproduct were observed upon increasing the substrate and base concentrations (Table 1 and SI: Figure S1). We isolated and characterized this reaction product using MS, NMR and single crystal X-ray analysis (Figure 1, SI: Table S1 and Figure S2), which showed that a double addition of ylide had occurred to yield **12**, a molecule with two cyclopropane rings.

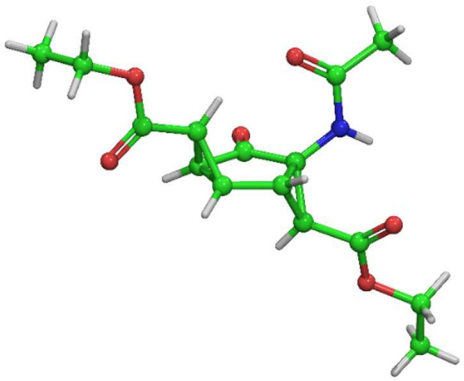

Figure 1. Crystal structure of **12**. The asymmetric unit contains both enantiomers (only one stereoisomer is shown here for clarity). Atom colors: carbon-green; nitrogen-blue; oxygen-red; hydrogen-white.

In particular, increasing the concentration of **8** to 0.1 M led to a small increase in the amount of **12** formed with a concomitant decrease in the quantity of **10** (Table 1, entry 2, SI: Figure S3). When only 1 equivalent of DBU and sulfonium bromide (at 0.08 M) was employed we observed that some starting material remained unreacted and the reaction still gave **12** (Table 1, entry 3, SI: Figure S3), an observation that suggests formation of **12** from **10** occurs competitively with the ylide addition to **8**. In the presence of excess DBU (Table 1, entry 4, SI: Figure S3), we observed no trace of **10**, which had been converted completely to **12**.

Table 1. Cyclopropanation product molar ratios as determined by ^{1}H-NMR examination of the crude reaction under various conditions.

entry	DBU (equiv)	**9** (equiv)	[**8**] (M)	molar ratio percentage (^{1}H-NMR)			
				8	**10**	**11**	**12**
1	1.2	1.2	0.08	-	40%	48%	12%
2	1.2	1.2	0.10	-	34%	47%	19%
3	1.0	1.0	0.08	7%	40%	45%	8%
4	1.7	1.2	0.10	-	-	68%	32%

The facile formation of **12** prompted us to expand on previous experimental[23,24] and computational[28] studies concerning the mechanism of this reaction. We utilized DFT computational methodology similar to that used by Janardanan and Sunoj in their computational study on the reactivity and diastereoselectivity of a panel of sulfur ylides with an acyclic α,β-unsaturated ketone.[28] We optimized the ground states and transition states (TS) for all diastereomeric additions of the sulfonium ylide to our substituted cyclopentenone (SI: Figure S4), the free energy profile of the betaine intermediates, and the deprotonation reaction of **10**, which gives **12** using GAUSSIAN 09 implemented density functional theory (DFT) at B3LYP631+G(d,p) level of theory in an implicit $CHCl_3$ solvent IEFPCM dielectric.

We started by calculating the relative energies of the four pathways (SI: path a, b, c, d, respectively; Chart S1-4) that could result in the formation of the four possible diastereomeric reaction products (**10**, **11**, **13**, **14**, Scheme 3). For simplicity, only one enantiomer of **8** is considered in the discussion below and additional schemes are displayed in Figure S4 (SI). Our calculations are based on the mechanism of sulfur ylide addition to enone involving a Michael addition, which occurs prior to elimination of the SMe_2 group, and this general reaction sequence is represented in Scheme 3. We considered four modes of addition to the enone, which would give the four *endo/exo syn/anti* stereoisomers described above.

The betaine nomenclature used in **Scheme 3** refers to the interacting faces during addition: *Si* or *Re* face of ylide—*Si* or *Re* face of enone **8**, followed by the orientation of the sulfur cation relative to the ring: cisoid (**c**) for SMe_2 group over the ring, transoid (**t**) for SMe_2 antiperiplanar to C4, and reactive transoid (**rt**) for SMe_2 antiperiplanar to C1 (the orientation required for SMe_2 elimination).

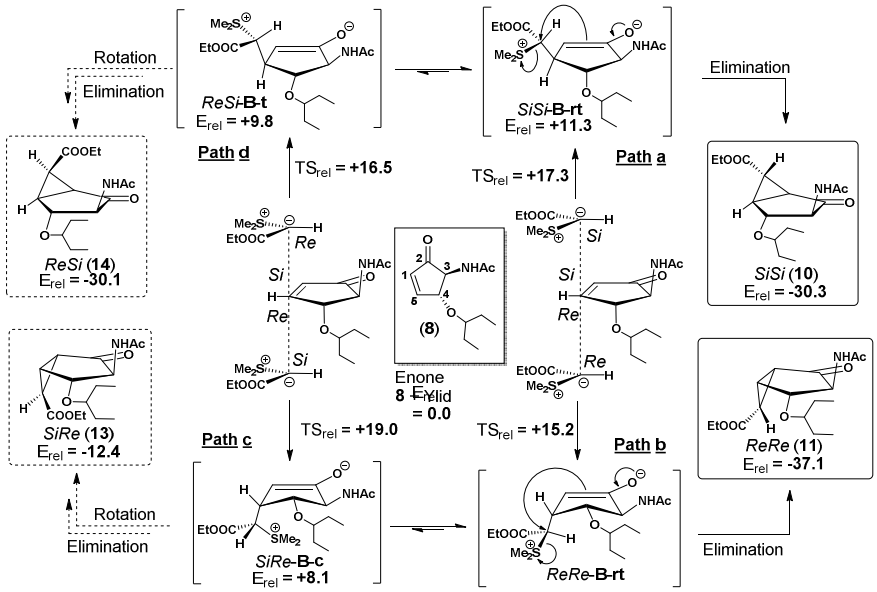

Scheme 3. Lowest energy addition for each diastereomeric pathway leading to either 'cisoid' betaines (**B-c**), 'transoid' betaines (**B-t**), or 'reactive transoid' betaines (**B-rt**), followed by reactions leading to cyclopropanated products. Energy barriers are given in kcal/mol relative to the ground state energy of the sulfur ylide + Michael acceptor **8** free in solution.

In order to identify the effect of steric encumbrance on facial selectivity, we performed multiple calculations by varying the orientation of the substituents during addition. Addition of the sulfur ylide to enone **8** to give a betaine intermediate, which is approximately 10–15 kcal/mol above the reaction ground state, is an endergonic process that is associated with calculated TS free energies barriers of around +15–20 kcal/mol (Figure 2a). The calculated optimized structure of **8** (Figure 2b) in solution has a C1–C5 π-

bond that restricts the motion of carbons C2-C1-C5-C4 (the dihedral angle for the C2-C1-C5-C4 dihedral is 1.6 degrees) allowing C3 to move out of the plane and position the NHAc in a pseudo equatorial orientation. In the betaine intermediate the π-bond restriction is between C1–C2 such that C5-C1-C2-C3 are approximately planar, with C4 out of the plane.

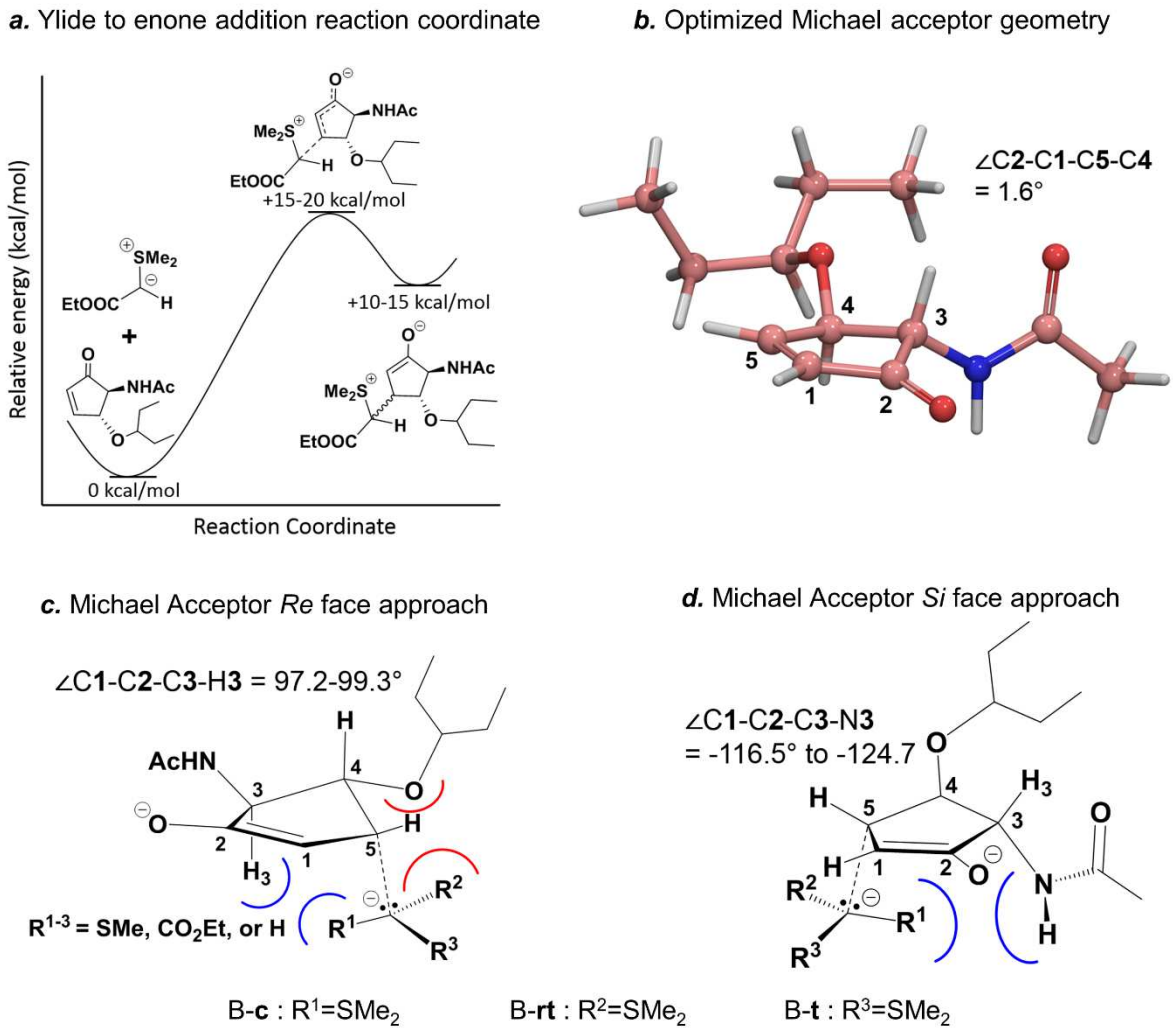

Figure 2. ***a.*** Reaction coordinate for addition of ylide to enone **8**. ***b.*** DFT optimized geometry for enone **8** geometry calculated in a chloroform dielectric. ***c.*** Addition of nucleophilic ylide to the *Re* face of the Michael acceptor, C4 is oriented out of the plane, into the opposite (*Si*) face of the Michael acceptor. ***d.***

Addition of nucleophilic ylide to *Re* face of the Michael acceptor, C4 is oriented out of the plane, into the opposite (*Re*) face of the Michael acceptor.

Addition to the *Re* face of the Michael acceptor (Figure 2c) necessitates that C4 moves in the opposite direction to the addition with the result that the pentan-3-yloxy group assumes a pseudo equatorial orientation. In contrast, Figure 2d displays the relative motions upon *Si* face addition, for example, the pentan-3-yloxy group is forced into an unfavorable axial orientation.

Clearly, steric crowding during ylide addition will be modulated by the relative orientation of the ylide to the cyclopentyl substituents (Figure 2c, d). When adding to the Si face, the least sterically hindered approach occurs when the sulfur ylide is oriented such that R_1 = H (Figure 2c, d). Indeed, having the smallest group in close proximity to NHAc group results in the lowest energy nucleophilic approach. When adding to the Re face, the lowest energy approach occurs for R_3 = COOEt, considering the unfavorable interactions with the axial H_3 and pentyloxy group associated with the R_1 and R_2 positions, respectively (Figure 2c).

Indeed, the two ylide-acceptor facial attacks with R_1 = H and R_3=COOEt (Figure 2) lead to the reactive transoid betaine **B-rt** conformations that undergo cyclopropanation readily to form the observed monocyclopropaned products (with *ReRe* and *SiSi* pro-chiral faces for the ylide-acceptor, Scheme 3: Path a,b). The TS of addition to form the reactive ReRe/SiSi betaine rotamers are lower in energy than the TSs to form the equivalent non-reactive rotamers, as well as the TS of addition for reactive ReSi/SiRe rotamers of unobserved products **13**/**14**. These reactive rotamers, in contrast, have higher energy TSs of addition than their non-reactive betaine rotamer counterparts (Scheme 3: Path c,d).

DFT studies reported by Janardanan et al.[28] on MIRC addition reactions involved the use of stabilized ylides on acyclic substrates. These authors concluded that following the first bond forming step the betaine intermediate that is lower in energy has the charged sulfur atom of the ylide adjacent to the

enolate oxygen, due to favorable electrostatic interactions. As a result, bond rotation, which positions the SMe_2 group opposite to the enolate fragment, is necessary for elimination.[9]

Considering the cyclic nature of the Michael acceptor, we calculated all three possible rotamers in order to rationalize why certain diastereomeric products are formed. Of note, the favorable electrostatic interactions between the sulfonium center and enolate are likely modulated by steric compression resulting from orienting the SMe_2 group over the ring. That is, although the ReRe-**B-rt** betaine has the lowest energy addition TS (E_{rel} = 15.2 kcal/mol), the betaine intermediate itself is not a local minimum as it spontaneously undergoes ring closing; all attempts to optimize the betaine intermediate structure resulted in cyclopropane **11**. This is likely due to the steric repulsion between the pentan-3-yloxy group and the SMe_2 substituent (Figure 3a); this interaction orients the ylide carbon closer to C1, lowering the barrier for SMe_2 elimination and formation of **11**.

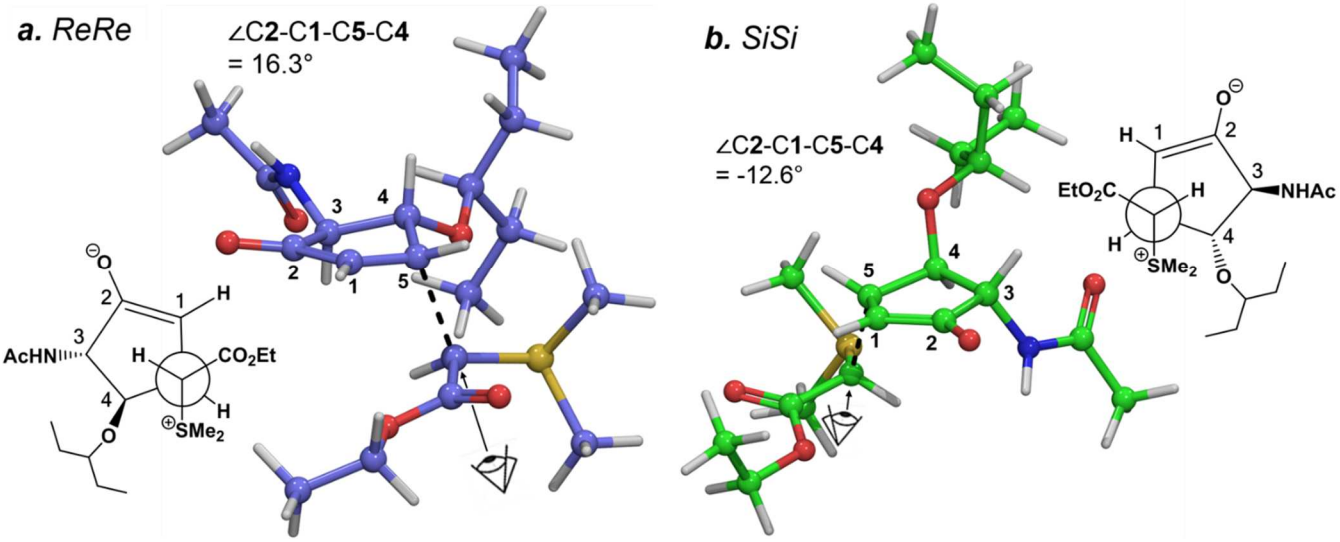

Figure 3: ***a.*** DFT optimized TS geometry for **B-rt** intermediate formation with the *Re* face of sulfur ylide nucleophile attacking the *Re* face of the acceptor. ***b.*** DFT optimized TS geometry for **B-rt** intermediate formation with the *Si* face of sulfur ylide nucleophile attacking the *Si* face of the acceptor.

This behavior is exemplified in visualizations of potential energy surfaces (PES) obtained by iteratively changing the dihedral angles and sulfur-ylide carbon bond distance (SI: Surface S1 and S2). PESs show that upon rotation from the **B**-**t** to the **B**-**rt** conformations for the *SiSi* betaine (DFT optimized TS geometry shown in Figure 3b), the **B**-**rt** structure sits in a small energy well, whereas for the *ReRe* betaine, no such local minima exists.

When direct formation of the reactive rotamer has a significantly higher barrier than the non-reactive rotamer, the indirect pathway to the reactive conformation needs to be considered. In path c (*SiRe*) and d (*ReSi*), the bulky COOEt group is positioned above the ring in the reactive **B-rt** conformation, causing considerable unfavorable steric and electrostatic interactions and causing the reactive rotamer to have the highest TS for addition. Because direct formation of reactive betaines **B-rt-13** and **B-rt-14** is disfavored, formation of the unreactive betaine rotamers will be much faster. These betaine intermediates then have multiple possible pathways: they can rotate to another betaine conformation, dissociate back into ylide and Michael acceptor, or epimerize to another diastereomer via deprotonation. In pathway c/d, the TSs for rotation between non-reactive conformers (**B-c** ↔ **B-t**) are lower than the TS for rotation to the reactive conformation ($E^{\ddagger}_{\mathbf{B-t} \leftrightarrow \mathbf{B-rt}} > E^{\ddagger}_{\mathbf{B-c} \leftrightarrow \mathbf{B-t}} < E^{\ddagger}_{\mathbf{B-c} \leftrightarrow \mathbf{B-rt}}$). If we evaluate these reactions using a Curtin-Hammett interpretation,[29] the product distribution should depend on the difference in energy between the interconverting pair of rotamers as well as the free energy of the TS for the irreversible reactions. For this case, the irreversible reactions are dissociation to starting material and rotation to the reactive conformation (Figure 4).

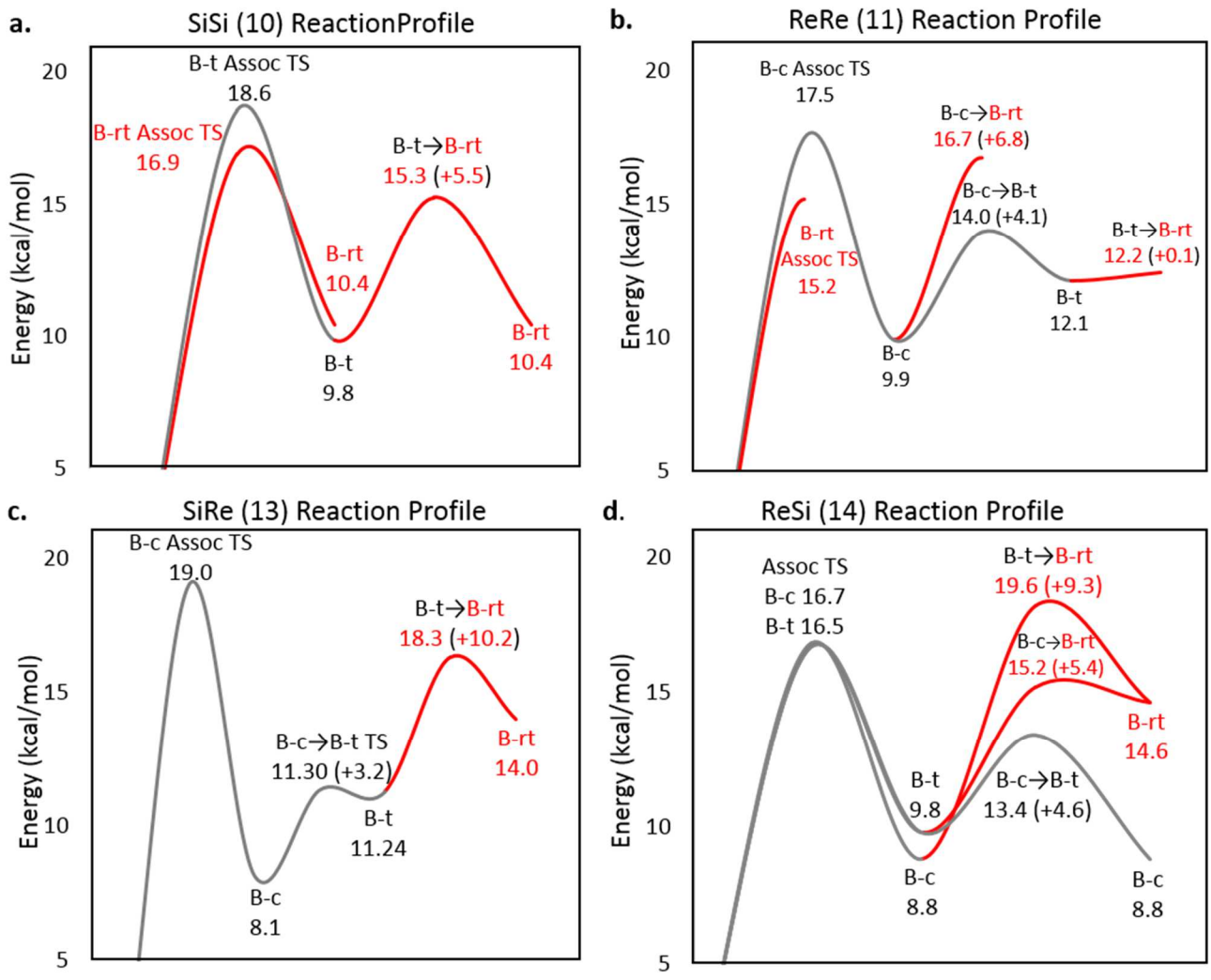

Figure 4. Reaction Profiles for each diastereomeric approaches: **a.** *Si* Ylide-*Si* Acceptor **b.** *Re* Ylide-*Re* Acceptor **c.** *Si* Ylide-*Re* Acceptor **d.** *Re* Ylide-*Si* Acceptor. Lowest energy addition TS (Assoc TS) barriers shown and rotation between non-reactive conformers cisoid (B-c) and transoid (B-t) betaines and rotation to the reactive transoid betaine (B-rt) conformation. Energies are given in kcal/mol based on the calculated zero-point energies of the TSs and betaine intermediates relative to the sum of ground state energies of the dissociated ylide **8** and Michael acceptor.

In paths a/b that lead to observed products **10/11**, there is little interconversion between intermediates because the barrier to the reactive conformation is significantly lower than that for intermediate

interconversion (Figure 4 and SI: SchemeS1). In paths c/d, there is interconversion between B-c and B-t due to the smaller barrier for interconversion between unreactive rotamers relative to the dissociation and rotation to B-rt. Considering that these two mechanistic pathways lead to unobserved products, but dissociation is 2.7 kcal/mol higher for path c and 1.3 kcal/mol for path d, these intermediates must be epimerizing instead of reacting to products **13/14** via paths c/d. We propose that the fate of these interconverting betaine intermediates is determined by equilibration caused by deprotonation and protonation of the proton alpha to SMe_2, resulting in conversion of these betaine intermediates to their epimers (as reported previously).[23] This equilibration would allow the *ReSi*/*SiRe* betaines to epimerize to the *SiSi*/*ReRe* betaine and rationalize the absence of products **13/14** in the reaction. The epimerization process also accounts for the energy difference between **B-rt** association TSs for the SiSi **10** and ReRe **11** products (which were determined experimentally to be in ~1:1 ratio, although the association TS for **B-rt-10** was 1.7 kcal/mol higher than **B-rt-11**).

Finally, we discuss the formation of compound **12**, which possesses two *exo*-cyclopropyl carboxylate esters that are on opposite sides of the original cyclopentenone ring. We performed a series of experiments (Table 1) with various concentrations and amounts of DBU and ylide. Our results are consistent with product **12** being derived from deprotonation of H_3 on the *SiSi* compound **10** (Scheme 4). That is, we propose that the formation of enolate **15** results in a facile β-elimination of pentan-3-olate to generate a new unsaturated ketone that is able to undergo another Johnson-Corey-Chaykovsky cyclopropanation to give **12**. Notably, **11** is unable to undergo this reaction because deprotonation of H_3 is sterically hindered by both the 3-pentylether and the cyclopropane ring (Scheme 4).

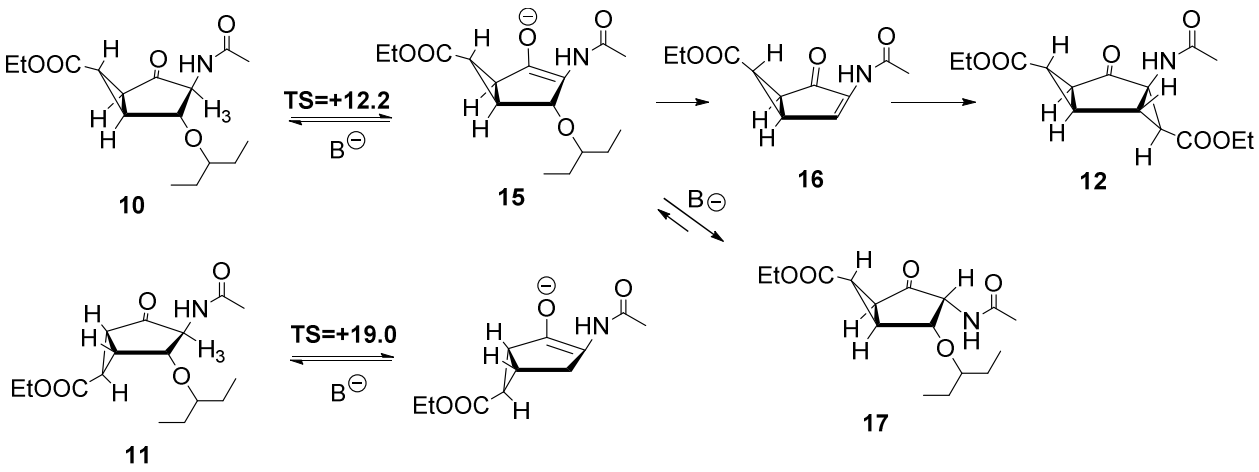

Scheme 4. Proposed reaction mechanism for the formation of **12** from **10**.

In presence of DBU, with higher enone concentrations (0.1 M, Table 1 entry 2), the bimolecular deprotonation/protonation of **10** is accelerated. In excess DBU (entry 4), compound **10** is converted completely to product **12**. Under these reaction conditions, the formation of compound **17** (Scheme 4), isolated by chromatography (isolated yield = 3%, SI: Figure S5 and Table S2), also supports the formation of enolate **15** from compound **10**. Transition state optimization for proton abstraction of SiSi compound **10** and *ReRe* compound **11** confirmed that the H_3 proton of compound **10** had a lower barrier for abstraction, with a TS 7 kcal/mol lower than the H_3 deprotonation TS of **11**. Furthermore, a scan was performed in which the distance of H_3 from the C_3 carbon (Figure 5) was incremented in steps of 0.05 angstrom once associated to a DBU molecule. During this scan, as the proton carbon distance increases, the optimization converges to a minimum in association with the pentan-3-yloxy oxygen (Figure 5). This suggests that when DBU deprotonates **10** it can readily associate with the pentan-3-yloxy oxygen, which is then primed for elimination. This does not occur with **11** because the cyclopropane ring causes steric crowding that not only raises the TS energy but also destabilizes association of protonated DBU.

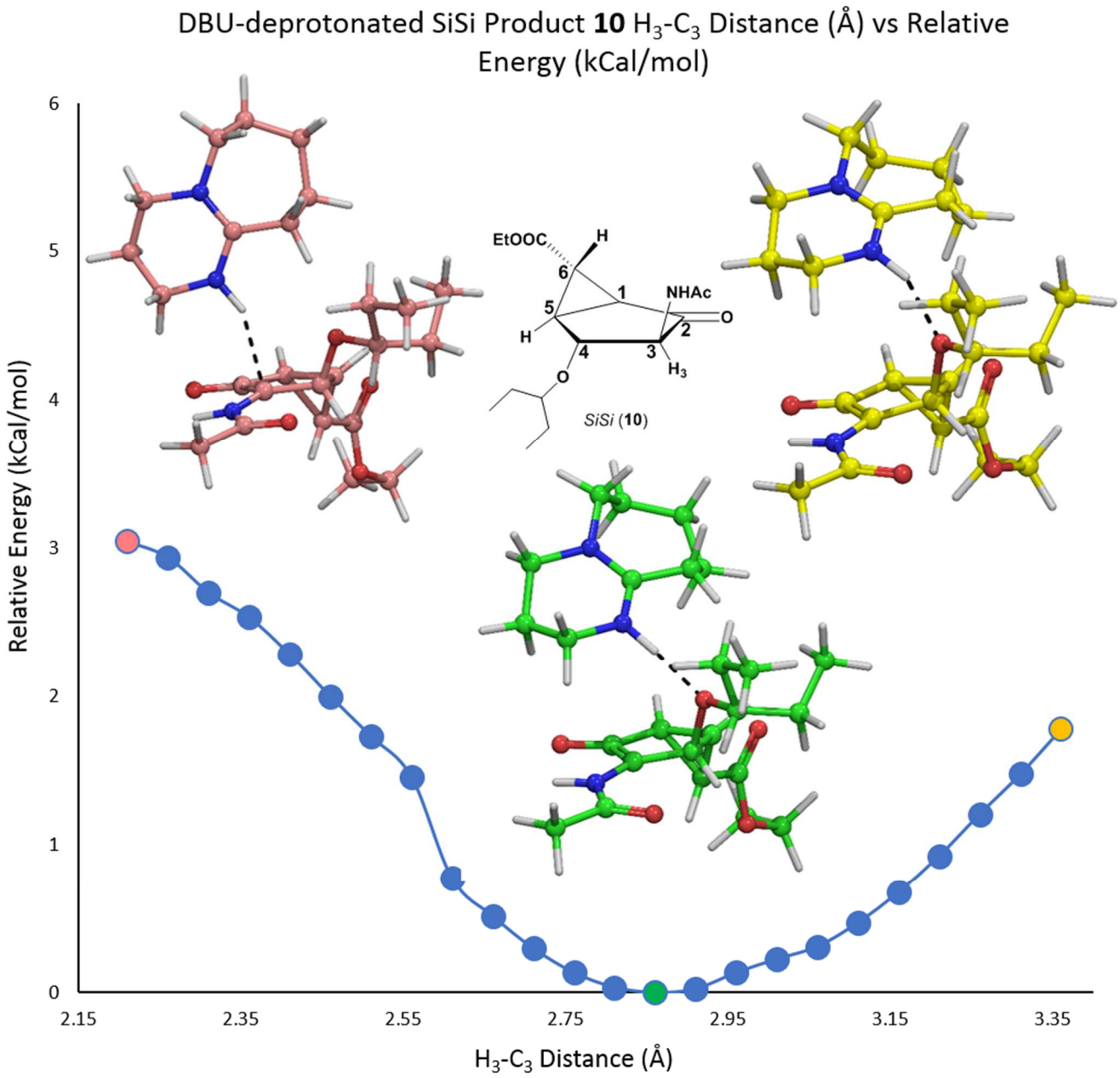

Figure 5. Protonated DBU C3-H3 distance scan with DFT using B3LYP 6-31G level of theory.

These data confirmed that the MIRC reaction with enone **8** in the presence of excess base ultimately led to the conversion of the *exo-anti* cyclopropyl product **10** to the tricyclic[4.1.0.$0^{2,4}$]heptane product **12** with both cyclopropylcarboxylate esters in *exo* configurations.

CONCLUSION

A functionalized cyclopentenone reacts in a MIRC reaction with a stabilized sulfonium ylide to give the corresponding *exo* cyclopropyl-cyclopentanes. This can be explained by the steric and electrostatic interactions arising during the C-C bond rotation, as well as from basic equilibration, allowing the sulfur group elimination. Interestingly, in the presence of excess base, one of the two bicyclic products converts completely into a tricyclic[4.1.0.$0^{2,4}$]heptane product with a double addition of cyclopropane. Theoretical calculations suggest that selective formation of **10** and **11** occurs due to the epimerization of unreactive intermediates from pathways leading to products **13** and **14**, as energy barriers for some of these intermediates are lower than that of the observed products. Formation of the tricyclic product was rationalized by calculating and comparing energy barriers for proton abstraction of products **10** and **11** required to form the intermediate precursor for second cyclopropanation. Of note, while bicyclo[3.1.0]hexane derivatives have been reported in the literature and gained much attention owing to their significance as glutamate receptor agonists/antagonists,[18] this novel tricyclic[4.1.0.$0^{2,4}$]heptane scaffold, appropriately functionalized, could find application as a conformationally constrained analogue of amino acids.

EXPERIMENTAL

General information. All chemicals were of analytical grade.^{1}H- and ^{13}C**{^{1}H}**-NMR spectra were acquired on a Bruker instrument and recorded at 500 MHz and 150 MHz, respectively. Spectra are reported as follows: chemical shift (δ ppm), multiplicity (s = singlet, d = doublet, t = triplet, q = quartet, quint = quintet, m = multiplet, bs = broad singlet), coupling constants (Hz). All assignments were confirmed with the aid of two-dimensional ^{1}H-^{1}H (COSY), ^{1}H-^{13}C (HSQC) and/or ^{1}H-^{13}C (HMBC) experiments using standard pulse programs. Processing of the spectra was performed using MestReNova software. Product numbering for spectral assignment is clarified in the Supporting Information.

Analytical thin-layer chromatography (TLC) was performed on aluminum plates pre-coated with silica gel 60F-254. The developed plates were air dried, exposed to UV light, and/or sprayed with a solution containing molybdic reagents or permanganate reagents, and heated. Column chromatography was performed with an automated flash chromatography system. High resolution mass spectra were obtained by the electrospray ionization method, using a TOF LC/MS high-resolution magnetic sector mass spectrometer. Melting points were measured with a SMP3 melting point apparatus.

General procedure for the cyclopropanation reaction. A solution of ethyl (dimethylsulfonium)acetate bromide **2** and DBU in $CHCl_3$ was stirred vigorously at room temperature for 30 min. Compound **8** dissolved in the minimum amount of $CHCl_3$ was added to the stirring mixture. The final concentration of substrate **8** is reported in Table 1. The reaction mixture was stirred overnight at room temperature (TLC 2:8 Hex:EtOAc; $KMnO_4$ stain), then diluted with $CHCl_3$ and washed with 0.1 M $NaHSO_4$, dried over sodium sulfate, filtered, and concentrated under vacuum. The residue was purified by column chromatography (from 70:30 Hex:EtOAc to 25:75 Hex:EtOAc in 20 column volume) to isolate **10**, **11**, **12**, **17** depending on the reaction conditions (TLC 2:8 Hex: EtOAc R_f (**8**) = 0.30, R_f (**17**) = 0.45, R_f (**11**) = 0.55, R_f (**12**) = 0.62, R_f (**10**) = 0.71, $KMnO_4$ stain).

Procedure (Table 1, entry 1): A solution of ethyl (dimethylsulfonium)acetate bromide **2**(140 mg, 0.607 mmol, 1.2 equiv) and DBU (93 µL, 0.607 mmol, 1.2 equiv) in $CHCl_3$ (5.8 mL) was stirred vigorously at room temperature for 30 min. Compound **8** (114 mg, 0.506 mmol, 1 equiv) dissolved in the minimum amount of $CHCl_3$ (500 µL) was added to the stirring mixture. The reaction mixture was stirred overnight at room temperature (TLC 2:8 Hex:EtOAc; $KMnO_4$ stain), then diluted with $CHCl_3$ and washed with 0.1 M $NaHSO_4$, dried over sodium sulfate, filtered, and concentrated under vacuum. The residue was purified by column chromatography (from 70:30 Hex:EtOAc to 25:75 Hex:EtOAc in 20 column volume) to isolate **10** (58 mg, yield = 37%), **11** (76 mg, yield = 48%), **12** (16 mg, yield = 10%).

Procedure (Table 1, entry 4): A solution of ethyl (dimethylsulfonium)acetate bromide **2** acetate (148 mg, 0.638 mmol, 1.2 equiv) and DBU (135 µL, 0.903 mmol, 1.7 equiv) in $CHCl_3$ (5.3 mL) was stirred vigorously at room temperature for 30 min. Compound **8** (120 mg, 0.531 mmol, 1 equiv) dissolved in the minimum amount of $CHCl_3$ (500 µL) was added to the stirring mixture. The reaction mixture was stirred overnight at room temperature (TLC 2:8 Hex:EtOAc; $KMnO_4$ stain), then diluted with $CHCl_3$ and washed with 0.1 M $NaHSO_4$, dried over sodium sulfate, filtered, and concentrated under vacuum. The residue was purified by column chromatography (from 70:30 Hex:EtOAc to 25:75 Hex:EtOAc in 20 column volume) to isolate **11** (102 mg, yield = 62%), **12** (48 mg, yield = 29%), **17** (5 mg, yield = 3%). Compounds 10 and 11 have been previously reported.[27] ^{1}H NMR data acquired in $CDCl_3$ are reported in the Supporting Information to allow a direct in comparison with compounds **12** and **17**, characterized in $CDCl_3$. Table S2 lists the assignment of ^{1}H-NMR coupling constants of the products.

Compound **12 diethyl (1RS,2SR,4RS,6SR)-4-acetamido-5-oxotricyclo[4.1.0.0^{2,4}]heptane-3,7-dicarboxylate**; colorless solid, mp =134–138 °C, ^{1}H NMR (500 MHz, $CDCl_3$) δ 6.24 (s, 1H, NH), 4.24-4.11 (m, 4H, $CH_{2\text{-Ethyl}}$), 3.17 (t, *J* = 3.1 Hz, 1H, H_6), 2.68 (dd, *J* = 4.0, 1.6 Hz, 1H, H_4), 2.54 (dd, *J* = 5.0, 3.4 Hz, 1H, H_1), 2.20 (dt, *J* = 5.0, 2.5 Hz, 1H, H_5), 2.14 (d, *J* = 4.0 Hz, 1H, H_7), 2.00 (s, 3H, $CH_{3\text{-Ac}}$), 1.12-1.40 (m, 6H, $CH_{3\text{-Ethyl}}$). ^{13}C{^{1}**H**}-NMR (150 MHz, $CDCl_3$) δ 202.7 (C_2), 171.6 (CO_{Ac}), 169.6 ($CO_{Ethyl\text{-}6}$), 167.4 ($CO_{Ethyl\text{-}7}$), 62.0 ($CH_{2Ethyl\text{-}7}$), 61.5 ($CH_{2Ethyl\text{-}6}$), 33.5 (C_4), 33.0 (C_7), 31.5 (C_5), 30.9 (C_6), 27.4 (C_1), 22.8 (C_{Ac}), 14.2 (CH_{3Ethyl}), 14.2 (CH_{3Ethyl}). HRMS (ESI) m/z: [M + H]+ Calcd for $C_{15}H_{20}NO_6$ 310.1291; Found 310.1285; m/z: [M + Na]+ Calcd for $C_{15}H_{19}NO_6Na$ 332.1110; Found 332.1105; m/z: [M + K]+ Calcd for $C_{15}H_{19}NO_6K$ 348.0849; Found 348.0844.

Compound **17 ethyl (1SR,3RS,4SR,5RS)-3-acetamido-2-oxo-4-(pentan-3-yloxy) bicyclo[3.1.0]hexane -6-carboxylate**; yellow oil, ^{1}H NMR (500 MHz, $CDCl_3$) δ 6.06 (d, *J* = 7.0 Hz, 1H, NH), 4.21-4.10 (m, 3H, H_4, CH_{2Ethyl}), 3.49 (dd, *J* = 7.0, 4.3 Hz, 1H, H_3), 3.44-3.37 (m, 1H, CH_{Ether}), 2.71 (t, *J* = 3.2 Hz, 1H, H_6), 2.53 (dd, *J* = 5.7, 2.9 Hz, 1H, H_1), 2.39 (dd, *J* = 5.7, 3.7 Hz, 1H, H_5), 1.99 (s, 3H,

CH_{3Ac}), 1.63-1.50 (m, 4H, $CH_{2\text{-}Ether}$), 1.27 (t, *J* = 7.1 Hz, 3H, $CH_{3\text{-}Ethyl}$), 0.95 (t, *J* = 7.4 Hz, 3H, $CH_{3\text{-}Ether}$), 0.88 (t, *J* = 7.5 Hz, 3H, $CH_{3\text{-}Ether}$). $^{13}C\{^{1}H\}$- NMR (150 MHz, $CDCl_3$) δ 204.5 (C_2), 171.1 (CO_{Ac}), 167.4 (CO_{Et}), 81.9 (CH_{Ether}), 81.7 (C_4), 61.1 (CH_{2Et}), 51.9 (C_3), 28.3 (C_5), 26.8 ($CH_{2\text{-}Ether}$), 26.5 ($CH_{2\text{-}Ether}$), 25.0 (C_1), 23.4 (C_{Ac}), 20.9 (C_6), 14.3 (CH_{3Et}), 9.9 ($CH_{3\text{-}Ether}$), 9.5 ($CH_{3\text{-}Ether}$). HRMS (ESI) m/z: [M + H]+ Calcd for $C_{16}H_{26}NO_5$ 312.1811; Found 312.1805; m/z: [M + Na]+ Calcd for $C_{16}H_{25}NO_5Na$ 334.1630; Found 334.1625.

Computational Methods. All structures were optimized using GAUSSIAN09 software suite, with Density Functional Theory (DFT) at B3LYP 6-31+G(d,p) level of theory and $CHCl_3$ solvation (ε = 4.7113) with a Polarizable Continuum Model (PCM) using the integral equation formalism variant (IEFPCM). Transition states for all possible diastereomeric additions of the sulfur ylide to the Michael acceptor were obtained using the QST3 Synchronous Transit-guided Quasi-Newton algorithm based on structures provided for reactant, product and transition state approximation. For betaine rotational TSs convergence using QST3 could not be obtained in all cases, thus, TS structures were obtained by performing small step rotational dihedral angle scanning at B3LYP 6-31+G(d,p) level of theory. The highest energy structure along the scan coordinate (along C1-C5 atoms of the acceptor, sulfur bearing carbon of the ylide and sulfur atom) was subjected to an optimization-frequency calculation (with the aforementioned rotational dihedral angle fixed) and we verified that the output had a negative frequency corresponding to the appropriate rotational TS. This technique was used for a rotational TS in which QST3 convergence was successful and the difference in energy between TS structures obtained was <0.06 kcal/mol. This same strategy was used to locate the TS for deprotonation of products **10** and **11**. Potential energy surfaces were made by running a two-parameter scan using the Gaussian with Hartree-Fock method. Energy values were extracted from the output files and plotted to a surface using MATLAB R2016b Delaunay triangulation and trisurf function. Calculated geometries displayed in figures were visualized using PyMOL.

AUTHOR INFORMATION

Corresponding Authors: bennet@sfu.ca; cinzia.colombo@unimi.it

Notes: The authors declare no competing financial interest.

ACKNOWLEDGMENTS

This work was supported by funding from the People Programme of the European Union's Seventh Framework Programme by a Marie Curie Outgoing Fellowship to C.C. under REA *grant agreement* n° PIOF-GA-2012-327579, by a Natural Sciences and Engineering Research Council of Canada (NSERC) Canadian Graduate Scholarship-Doctoral (M. F.-D.), a NSERC Discovery Grant (AJB: #121348-2012) and a Canadian Institutes of Health Research operating grant (AJB, MOP-259122).

ASSOCIATED CONTENT

Supporting Information: The Supporting Information is available free of charge on the ACS Publications website at DOI:. ^{1}H and ^{13}C NMR spectra of all new compounds and reaction mixtures, structural details for compound 12, and reaction pathways studied theoretically, calculated energies, and contour plots (PDF).

REFERENCES

(1) Chen, D. Y. K.; Pouwer, R. H.; Richard, J.-A. *Chem. Soc. Rev.* **2012**, *41*, 4631.

(2) Doyle, M. P.; Forbes, D. C. *Chem. Rev.* **1998**, *98*, 911.

(3) Harvey, J. E.; Hewitt, R. J.; Moore, P. W.; Somarathne, K. K. *Pure Appl. Chem.* **2014**, *86*, 1377.

(4) Pellissier, H. *Tetrahedron* **2008**, *64*, 7041.

(5) Charette, A. B.; Juteau, H.; Lebel, H.; Molinaro, C. *J. Am. Chem. Soc.* **1998**, *120*, 11943.

(6) Muller, P.; Fernandez, D.; Nury, P.; Rossier, J. C. *Helv. Chim. Acta* **1999**, *82*, 935.

(7) Doyle, M. P. *J. Org. Chem.* **2006**, *71*, 9253.

(8) Itagaki, M.; Masumoto, K.; Yamamoto, Y. *J. Org. Chem.* **2005**, *70*, 3292.

(9) Lebel, H.; Marcoux, J. F.; Molinaro, C.; Charette, A. B. *Chem. Rev.* **2003**, *103*, 977.

(10) Aggarwal, V. K.; Fulton, J. R.; Sheldon, C. G.; de Vicente, J. *J. Am. Chem. Soc.* **2003**, *125*, 6034.

(11) Li, A. H.; Dai, L. X.; Aggarwal, V. K. *Chem. Rev.* **1997**, *97*, 2341.

(12) Burtoloso, A. C. B.; Dias, R. M. P.; Leonarczyk, I. A. *Eur. J. Org. Chem.* **2013**, *2013*, 5005.

(13) Johnson, A. W.; LaCount, R. B. *J. Am. Chem. Soc.* **1961**, *83*, 417.

(14) Corey, E. J.; Chaykovsky, M. *J. Am. Chem. Soc.* **1965**, *87*, 1345.

(15) Corey, E. J.; Chaykovsky, M. *J. Am. Chem. Soc.* **1965**, *87*, 1353.

(16) Deng, X. M.; Cai, P.; Ye, S.; Sun, X. L.; Liao, W. W.; Li, K.; Tang, Y.; Wu, Y. D.; Dai, L. X. *J. Am. Chem. Soc.* **2006**, *128*, 9730.

(17) Huang, K.; Huang, Z. Z. *Synlett* **2005**, 1621.

(18) Monn, J. A.; Valli, M. J.; Massey, S. M.; Wright, R. A.; Salhoff, C. R.; Johnson, B. G.; Howe, T.; Alt, C. A.; Rhodes, G. A.; Robey, R. L.; Griffey, K. R.; Tizzano, J. P.; Kallman, M. J.; Helton, D. R.; Schoepp, D. D. *J. Med. Chem.* **1997**, *40*, 528.

(19) Rasmy, O. M.; Vaid, R. K.; Semo, M. J.; Chelius, E. C.; Robey, R. L.; Alt, C. A.; Rhodes, G. A.; Vicenzi, J. T. *Org. Process Res. Dev.* **2006**, *10*, 28.

(20) Sun, X. L.; Tang, Y. *Acc. Chem. Res.* **2008**, *41*, 937.

(21) Yamada, S.; Yamamoto, J.; Ohta, E. *Tetrahedron Lett.* **2007**, *48*, 855.

(22) Johnson, C. R.; Schroeck, C. W. *J. Am. Chem. Soc.* **1971**, *93*, 5303.

(23) Riches, S. L.; Saha, C.; Filgueira, N. F.; Grange, E.; McGarrigle, E. M.; Aggarwal, V. K. *J. Am. Chem. Soc.* **2010**, *132*, 7626.

(24) Aggarwal, V. K.; Grange, E. *Chem.-Eur. J.* **2006**, *12*, 568.

(25) Ruano, J. L. G.; Fajardo, C.; Martin, M. R.; Midura, W.; Mikolajczyk, M. *Tetrahedron Asymm.* **2004**, *15*, 2475.

(26) Romo, D.; Meyers, A. I. *J. Org. Chem.* **1992**, *57*, 6265.

(27) Colombo, C.; Pinto, B. M.; Bernardi, A.; Bennet, A. J. *Org. Biomol. Chem.* **2016**, *14*, 6539.

(28) Janardanan, D.; Sunoj, R. B. *J. Org. Chem.* **2007**, *72*, 331.

(29) Seeman, J. I. *Chem. Rev.* **1983**, *83*, 83.